Ground-State Proton Transfer of 7-Hydroxyquinoline Confined in Biologically Relevant Water Nanopools

Sun-Young Park, Oh-Hoon Kwon,[†] Taeg Gyum Kim,[‡] and Du-Jeon Jang*

School of Chemistry, Seoul National University, NS60, Seoul 151-742, Korea

Received: April 22, 2009; Revised Manuscript Received: July 27, 2009

The ground-state reverse proton transfer of 7-hydroxyquinoline catalyzed by water confined in AOT reverse micelles has been investigated by measuring time-resolved transient-absorption spectra and kinetic profiles. The transfer time is profoundly retarded in water nanopools compared with that in bulk water (26 μs) although it diminishes with the size increase of the water nanopool. The spectral-shift time of tautomeric transient absorption agrees well with the proton transfer time. The probe molecule is subject to the local gradient of polarity, whose magnitude is altered with the sizes of water nanopools. Accordingly, the observations made in this study indicate the multidimensional character of reaction coordinates, in which solvent polarization coupled to charge transfer plays a seminal role in the control of overall proton-transfer dynamics. The retardation of proton transfer in water nanopools is ascribed to the increased formation energy of a charge-transferred optimal configuration, which is prerequisite to facile intrinsic proton transfer via tunneling.

1. Introduction

Due to its key role in a variety of biological and chemical phenomena, proton transfer attracts considerable attention.[1−11] In particular, proton transfer in water has been extensively investigated because of its fundamental importance.[2−4] Water itself in the gas phase has low proton affinity compared with other proton acceptors,[12,13] whereas bulk water possesses great proton affinity due to the formation of extensive hydrogen (H)-bond networks. The dynamics and the mechanism of excited-state proton transfer (ESPT) in water have been widely studied with diverse photoacids.[2−4,11,14−21] Their strong acidity can be turned on by photoexcitation to yield a fast pH jump as a consequence, which is followed by proton diffusion and recombination. Aromatic molecules having both acidic and basic functional groups are interesting because they may serve as experimental models to study the proton relay of enzymes, ion channels, and spanning membrane proteins.[5−7] In this regard, hydroxyquinolines and their derivatives, having two prototropic groups of enol and imine, are extensively explored.[22−41] The enolic and the imino groups of 3-, 6-, and 7-hydroxyquinoline become much more acidic and basic, respectively, in S_1 than in S_0.[8,32−38] Because the proton donor and acceptor groups are distal to each other, ESPT to undergo tautomerization can occur with the assistance of protic solvent molecules, thus reflecting the nature of the solvent environment. The hydroxyquinolines are known to undergo the excited-state tautomerization of enol deprotonation and imine protonation stepwise in bulk water via forming anionic intermediate species.[34−39] On the other hand, 7-hydroxyquinoline (7HQ) in nonaqueous protic solvents such as alcohols is known to form a H-bond chain, along which proton relay can take place.[22−32] Solvent reorganization prior to intrinsic proton transfer to form an appropriate configuration for proton transfer is crucial in the dynamics of proton relay.[32,33]

In physiological systems, water is often contained in a small pocket of a membrane. The confinement effect in nanopools and enclosing interfacial surfaces can regulate water properties, such as H-bonding ability and polarity, which are the key elements of proton transfer in water. It is requisite, therefore, to explore a biologically important process of proton transfer closely in biologically relevant aqueous model systems for better understanding of water in living organisms. Among the model systems are reverse micelles, which are formed by surfactant molecules having polar headgroups pointing inward and dispersed in hydrocarbon solvents. Thus, water nanopools confined in reverse micelles serve as good mimic systems of biologically confined water molecules.[42−45] A distinguished feature of reverse micelles is their ability to make nonpolar solvents solubilize a large amount of water by encapsulating water nanopools in their inner polar cores.[46] About 20 molecules of surfactant Aerosol-OT (sodium 1,4-bis-2-ethylhexylsulfosuccinate, AOT) form a reverse micelle having a radius of 1.5 nm above the critical concentration of 1 mM in a hydrocarbon solvent.[47] The gradual addition of water to an AOT solution forms microemulsions of nanometer-sized water droplets surrounded by AOT molecules. In *n*-heptane, the radii in nanometers of the water nanopools are about $0.15w_0$, where w_0 is the molar ratio of water to AOT.[48] Water molecules at interfacial peripheries are strongly bound to the ionic headgroups of surfactant molecules while those at micellar cores are relatively free.[43] Thus, it is well-known that the structure, dynamics, and physicochemical properties of water molecules confined in a nanometer-sized space are greatly different from those of bulk water. The structures of AOT reverse micelles[48−50] and the solvation dynamics and the dielectric relaxation of water inside reverse micelles[47,51−56] have also been studied with diverse spectroscopic methods and molecular-dynamics simulations. It is reported that the mobility of water and dye molecules inside reverse micelles increases gradually with w_0 increment.[28,29]

Whereas ESPT dynamics in the reverse micelles has been widely explored for several photoacids,[33,45] because of experimental difficulty and explanatory intricacy, ground-state proton transfer (GSPT) dynamics has been rarely revealed regardless

* To whom correspondence should be addressed. E-mail: djjang@snu.ac.kr. Phone: +82-(2)-875-6624. Fax: +82-(2)-875-6624.

[†] Present address: Arthur Amos Noyes Laboratory of Chemical Physics, California Institute of Technology, Pasadena, CA 91125.

[‡] Present address: Samsung Electro-Mechanics Co., Suwon 443-743, Korea.

10.1021/jp903693f CCC: $40.75
Published on Web 08/13/2009

SCHEME 1: GSPT of 7HQ in Reverse Micelles

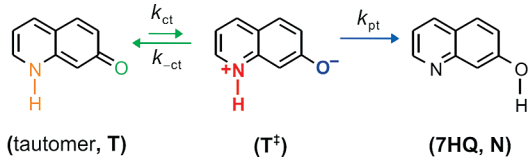

of its relevance to common prototropic processes in biological systems. In this paper, we report the GSPT dynamics of the tautomer (T) of 7HQ, transformed from the 7HQ normal species (N) via ESPT upon excitation, in confined water nanopools of AOT reverse micelles. As shown in Scheme 1, it is found that the reverse GSPT of 7HQ in water nanopools is coupled to the intramolecular charge transfer (k_{ct}) of keto equilibrium species T to form a zwitterionic optimal configuration ($T^{\ddagger}$), which is energetically unfavorable in a water nanopool with reduced polarity. Both the acidity of the N−H group and the basicity of the C═O group are suggested to increase by the charge transfer. Subsequently, intrinsic proton transfer (k_{pt}) catalyzed by water takes place to replenish N, which has been depleted upon photoexcitation. Equilibrium (k_{ct}/k_{-ct}) between charge transfer and back charge transfer (k_{-ct}) is considered to be rapid relative to k_{pt}. The observed rate constant (k_{PT}) is expressed as $(k_{ct}/k_{-ct})k_{pt}$. In a realistic static viewpoint, $k_{PT} = k_{pt} \exp(-\Delta G^{\ddagger}/RT)$ according to the transition-state theory,[17,57] where $\Delta G^{\ddagger}$ is the Gibbs free energy difference between the prevalent charge-delocalized T and the activated zwitterionic $T^{\ddagger}$. Thus, solvation-coupled charge transfer for the achievement of an appropriate electronic configuration is found to be prerequisite to efficient proton tunneling at the ground state.

2. Experimental Section

2.1. Materials. 7HQ (s, 99%), purchased from Acros, was further purified via column chromatography and vacuum sublimation. AOT (s, >99%) was used as received from Sigma-Aldrich, and *n*-heptane (l, >99%), purchased from Merck, was distilled once and stored over molecular sieves of 4 Å until use. 0.2 mM of 7HQ in AOT micelles was prepared by dissolving 2.9 mg of 7HQ in a 100 mL solution of 0.09 M AOT in *n*-heptane. In our samples, practically no more than one 7HQ molecule can be present in an AOT micelle consisting of 20 AOT molecules because [7HQ]/[micelle] is 0.04. Then a requisite amount of triply deionized water was added to the AOT solution to control w_0. To study the ^{2}H transfer of 7^{2}HQ, ^2H_2O (isotopic purity ≥99.9%, Sigma-Aldrich) in place of ^1H_2O was added to the AOT solution. All our samples were transparent and monodisperse throughout the experiments.

2.2. Measurements. While absorption spectra were measured with a UV/vis spectrophotometer (Scinco, S-2040), fluorescence spectra were obtained by using a home-built fluorometer consisting of a Xe lamp of 75 W (Acton Research, XS432) with a monochromator of 0.15 m (Acton Research, Spectrapro 150) and a photomultiplier tube (Acton Research, PD438) attached to a monochromator of 0.30 m (Acton Research, Spectrapro 300). Fluorescence spectra were not corrected for the wavelength-dependent sensitivity variation of the detector. Microsecond transient-absorption kinetic profiles were obtained by monitoring transmittance changes of a Xe lamp (Spectral Energy, LH150) beam of 75 W passing through an Ar-purged sample, which was excited at 337 nm with a N_2 laser (Laser Photonics, LN1000) having a pulse duration of 0.6 ns. The probe beam, wavelength-selected by using a monochromator of 0.25 m (Kratos, GM252) and a double monochromator of 0.2 m (Kratos, GM200), was detected with a photomultiplier tube (Hamamatsu, R928) and recorded with an oscilloscope of 200 MHz (Tektronics, TDS350). The kinetic profiles were collected every 5 nm to generate time-resolved transient absorption spectra. All the measurements were carried out at room temperature.

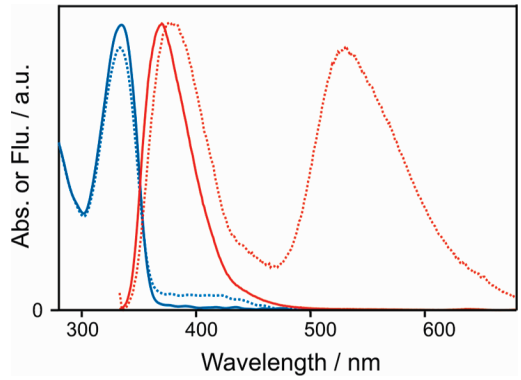

Figure 1. Absorption spectra (blue) and maximum-normalized fluorescence spectra with excitation at 330 nm (red) of 7HQ in AOT reverse micelles having $w_0 = 0$ (solid) and 12 (dotted).

3. Results

3.1. Steady-State Spectra. While the absorption spectrum of 7HQ in water-free ($w_0 = 0$) AOT reverse micelles shows only a normal absorption band at 331 nm, that in water-added reverse micelles displays an additional weak T absorption band at 410 nm (Figure 1). This indicates that T as well as N exists at the ground state in confined water nanopools.[34,38] As water concentration increases, T absorption grows gradually whereas N absorption decreases concomitantly.[33,38] In comparison with bulk aqueous solutions, equilibrium between N and T is obviously shifted toward N in confined water nanopools to become similar to that in alcoholic media: the micropolarity of water near 7HQ is substantially low compared with that in bulk water.[27,33]

In the absence of water ($w_0 = 0$), the emission spectrum of 7HQ in AOT micelles shows a single N* fluorescence band at 370 nm. In the presence of water ($w_0 = 12$), it shows an additional T* fluorescence band at 530 nm as well as the N* band at 380 nm (Figure 1). In comparison with the T* emission spectrum of 7HQ in bulk water,[33] that in water nanopools of AOT reverse micelles is bathochromically shifted by 20 nm. The spectral shift of N* emission from that in water-free AOT micelles and the red shift of T* emission from that in bulk water also suggest that the environment of 7HQ in water nanopools of AOT reverse micelles is very close to that in alcohols in polarity.[33] As the relaxation of T*, converted from N* via ESPT, generates T whose population is above its equilibrium concentration at the ground state, the depletion kinetics of T to replenish the photodepleted species of N reveals the dynamics of the reverse GSPT of 7HQ (see below).

3.2. Time-Resolved Transient-Absorption Spectra. In Figure 2, time-resolved transient-absorption spectra of 7HQ in water nanopools of AOT reverse micelles show a transient absorption band at 410 nm and an absorption bleach band at 330 nm with an isosbestic point around 370 nm; the cross point between two spectra changes are due to time-dependent spectral shift (see below). The transient absorption band is due to the ground-state formation of T while the bleach band is due to the ground-state depletion of N. N absorption bleach recovers concomitantly with the decay of T transient absorption. This indicates that transient T tautomerizes via GSPT to form N without ac-

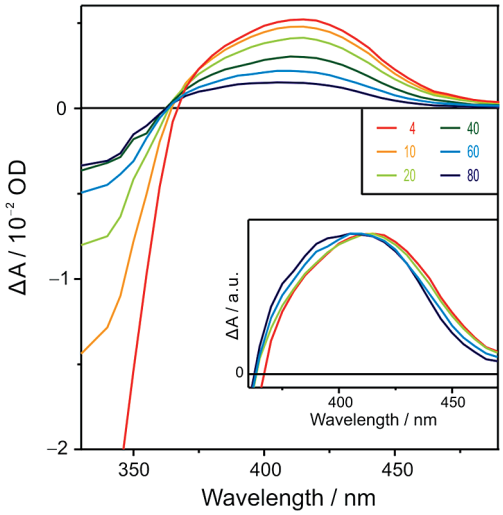

Figure 2. Time-resolved transient-absorption spectra (inset: maximum normalized) of 7HQ in AOT reverse micelles having $w_0 = 12$. The sample was excited at 337 nm and time delays after excitation are indicated inside in units of microseconds.

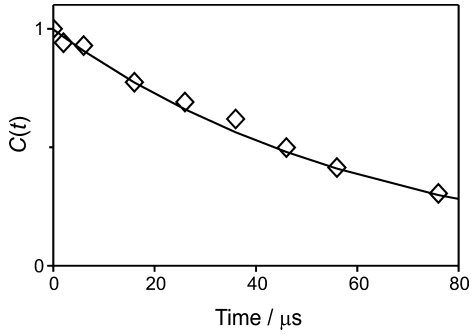

Figure 3. $C(t)$ decay kinetic profile of 7HQ in AOT reverse micelles having $w_0 = 12$ of ^1H_2O with excitation at 337 nm. The solid line denotes the best exponential decay fit with a time constant of 62(±3%) μs.

cumulating any intermediate species. Note that the transient absorption spectrum of T shifts gradually to the blue as time goes by (see the inset of Figure 2).

3.3. Spectral-Shift Correlation Function. The time-dependent spectral shift of transient T absorption can be analyzed by using the normalized spectral-shift correlation function of $C(t)$, defined as

$$C(t) = \frac{\nu(t) - \nu(\infty)}{\nu(0) - \nu(\infty)} \quad (1)$$

The $\nu(t)$, $\nu(0)$, and $\nu(\infty)$ of eq 1 are the frequencies of transient absorption at time delays of t, 0, and ∞, respectively, after photoexcitation. We have estimated $\nu(0)$ or $\nu(t)$ by averaging the frequencies at the blue and the red half maxima of the transient T absorption spectrum at a time delay of 0 or t. The value of $\nu(\infty)$ was estimated by fitting experimental data to an exponential function.[58] Figure 3 shows that a single-exponential decay with a time constant of 62 μs fits the $C(t)$ profile at $w_0 =$ 12 well and that the total shift, $\nu(0) - \nu(\infty)$, is 420 cm^{-1}. The total shift observed at the ground state is small compared with reported values (~2000 cm^{-1}) of other polar probe molecules at excited states.[49,50] On the other hand, the observed spectral-shift time is comparable to the GSPT time (56 μs) of 7HQ at the same value of w_0 (Figure 4 and Table 1). Since the spectral

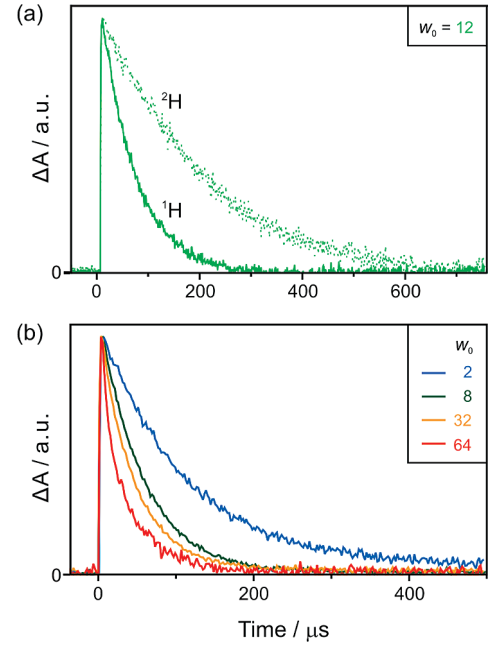

Figure 4. Transient-absorption kinetic profiles of 7HQ in AOT reverse micelles with variation of isotope (a) and w_0 (b). Samples were excited at 337 nm and transient absorption was monitored at 410 nm. The isotopes of protic hydrogen atoms and the values of w_0 are indicated inside.

TABLE 1: Transient-Absorption Time Constants and KIE of 7HQ in AOT Reverse Micelles at Various w_0 of ^1H_2O and ^2H_2O, Monitored at 410 nm upon Excitation at 337 nm

	decay time[a]/μs		
w_0	in ^1H_2O	in ^2H_2O	KIE[b]
2	115	370	3.2
4	74	238	3.2
8	56	180	3.2
12	56	181	3.2
16	54	175	3.2
20	54	174	3.2
24	52	167	3.2
28	51	165	3.2
32	48	160	3.3
40	46	153	3.3
48	43	144	3.4
64	37	129	3.5
∞[c]	26	80	3.1

[a] Relative errors are within ±2%. [b] Relative errors are within ±4%. [c] AOT-free bulk water.

shift of a solute is often coupled to solvent polarization (solvation), coincidence between the spectral-shift time and the overall GSPT time suggests the involvement of solvation-coupled charge transfer in the ground-state reverse tautomerization reaction (see below).

3.4. Transient-Absorption Kinetic Profiles. The transient-absorption kinetic profiles of T at various w_0 values fit well to single-exponential decay curves. Since the decay time of T matches with the recovery time of N, the reciprocals of observed time constants correspond to the overall GSPT rate constants of k_{PT}. Figure 4a, for example, displays the transient absorption kinetic profiles of T with the decay time constants of 56 and 181 μs at $w_0 = 12$ of ^1H_2O and ^2H_2O, respectively. Accordingly, the kinetic isotope effect (KIE) of the k_{PT} of GSPT is deduced to be 3.2, which is similar to that in bulk water (3.1)[37] and much greater than that of ESPT (1.5) for 7HQ in reverse micelles at $w_0 = 12$.[33] The large value of KIE suggests that a considerable

energy barrier and a significant tunneling contribution exist in the intrinsic proton transfer of GSPT in AOT reverse micelles. The unusually larger tunneling effect on the GSPT of 7HQ in bulk water already has been described in detail.[37] The transient-absorption decay of T becomes faster with w_0 increment in AOT reverse micelles (Figure 4b and Table 1). Note that even the decay time (37 μs) at the largest experimental w_0 of 64 in AOT micelles cannot reach that (26 μs) in bulk water. This agrees with the fact that water activity around 7HQ in confined water nanopools is considerably lower than that in bulk water.[59] The strong dependency of the overall reaction rate constant (k_{PT}) and the independency of KIE on w_0 imply the existence of multidimensional reaction coordinates including intrinsic proton transfer.

4. Discussion

In the nanopool of a reverse micelle, water molecules are roughly classified into two types: "bound water" and "free water".[43,44] Bound water molecules in the interfacial peripheries of water nanopools are regarded as immobile with low dielectric property because of strong binding to the headgroups of AOT. Free water molecules in the core of water pools have been reported to be mobile and polar almost like water in bulk.[33] The partition of a probe molecule depends on the electronic property of the molecule. For example, 2-naphthol prefers to dissolve in the headgroup region of reverse micelles, whereas its anion is found to be in the bound-water layer.[42] A charged anionic species can be fully embedded in the free-water cores at $w_0 \geq 12$ because of electrostatic repulsion by the anionic headgroup of AOT. N, on one hand, has been reported to reside primarily in the bound-water layer due to its moderate dipolar character.[33] On the other hand, the zwitterionic species of $T^{\ddagger}$ exists preferentially in the free-water core.[33] Considering that fluorescence from T* upon Franck−Condon excitation (520 nm) is in the middle of fluorescence from N*-tautomerized T* (530 nm) and that from T* in bulk water (510 nm),[33] we suggest that the keto species of T, tautomerized from N upon excitation, locates at an intermediary position between bound-water and free-water regions.

We now discuss the diffusion of a probe molecule within water nanopools on the time scale of GSPT (μs). The translational diffusion coefficient (D) of a probe can be estimated according to the Stokes−Einstein equation, $D = kT(6\pi\eta a)^{-1}$, where k is the Boltzmann constant, T is temperature, η is the viscosity of a medium, and a is the hydrodynamic radius of a solute. The a of 7HQ is assumed to be 4 Å because the van der Waals size of naphthalene is reported to be 6.8 × 5.1 Å^2. With $\eta = 44$ cP for water nanopools at $w_0 = 4$, D is calculated to be 1.2×10^{-11} m^2 s^{-1}. Therefore, the probe molecule of 7HQ can travel the root-mean-square distance [$(4Dt)^{1/2}$] of 0.6 nm (the radius of a water pool at $w_0 = 4$) on the time scale of 7 ns. For comparison, a 7HQ molecule at $w_0 = 40$ can diffuse the distance of 6.0 nm (the radius of a water pool in this case) on the time scale of 200 ns. These estimations hint that the time scale of molecular diffusion is not relevant to that of GSPT and that the keto solute of T can migrate from the less-polar bound-water region to the more-polar core region readily within the GSPT time to transform into the zwitterionic species of $T^{\ddagger}$.

We have shown that k_{PT} in AOT reverse micelles increases with w_0 increment (Figure 4 and Table 1). To understand the nature of this, we have also plotted the microviscosity of H_2O near 7HQ molecules as a function of w_0 (Figure 5). The microviscosity of water nanopools decreases with the increase of w_0. Compared with the microviscosity of water in bulk, that

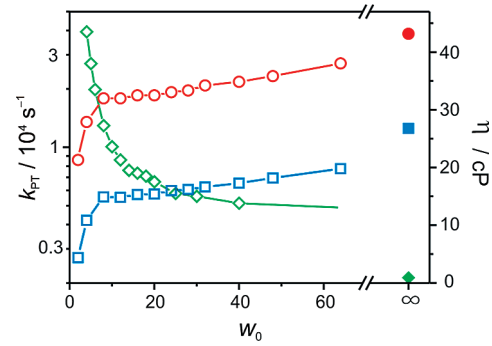

Figure 5. GSPT rate constant of 7^1HQ (circles) and 7^2HQ (squares) and microviscosity (η) of ^1H_2O (diamonds) versus w_0 in AOT water nanopools. The viscosity values were taken from ref 60, and we note that the viscosity of ^2H_2O is higher by 24% at room temperature than that of ^1H_2O.[62]

in AOT micelles is reported to be very large at low w_0 (40 cP at $w_0 = 4$). The viscosity decreases with w_0 increase, rapidly below $w_0 = 10$ and gradually above $w_0 = 10$.[60] Both the translational and the rotational motions of water are strongly suppressed in the confined nanopools because of geometrical confinement.[29,53,54] Thus, the mobility of water molecules increases with w_0 increment. The k_{PT} of the proton transfer of T increases conversely with the decrease of water viscosity. It is well-known that both the translational and the rotational diffusion constants of a probe molecule solubilized in confined water pools are inversely proportional to the viscosity of the solvent.[60] However, note that the observed proton transfer time of T (k_{PT}^{-1}) is larger by 10^5 times than the reported rotational diffusion time (τ_D) of T in AOT reverse micelles at the same w_0.[29] Although τ_D becomes as long as 200 ns for a large molecule of hemoglobin,[61] it is always enormously shorter than τ_{PT}. These suggest that solvent structural dynamics such as diffusion and reorientation is not directly related to the GSPT dynamics of 7HQ in reverse micelles, although it contributes to the dynamics of GSPT in a certain way.

Water in AOT reverse micelles has been suggested to be alcohol-like in polarity. In the confined water of reverse micelles having relative dielectric constants (ε) of 30−40, which are very close to ε of methanol (33) and much smaller than ε of bulk water (78),[43,44] the barrier of proton transfer increases extensively, because the local electric field depending on the location of a probe molecule influences the energetics of polar reactions such as proton transfer. There are two possible prototropic tautomers of 7HQ: the keto species of T and the zwitterionic species of $T^{\ddagger}$. Whereas $T^{\ddagger}$ is stable in bulk water,[37] T is present in alcohols such as methanol at the ground state.[23,24] While the acidity of the N−H group of $T^{\ddagger}$ is much larger than that of T, the basicity of the C═O group of $T^{\ddagger}$ is also enormously larger than that of T in nature. Because T is more stable than $T^{\ddagger}$ at small ε, the barrier of proton transfer via N−H deprotonation and C═O protonation concertedly or stepwise increases substantially with w_0 decrement. The zwitterionic configuration of $T^{\ddagger}$, essential for facile GSPT, is energetically unfavorable in confined water nanopools. Thus, only a small fraction of 7HQ molecules in water nanopools possess the optimal configuration of $T^{\ddagger}$ at the ground state. The k_{PT} increases with the size of the water nanopool (Table 1). Of note is that k_{PT} remains significantly smaller than that in bulk water. This agrees with the fact that 7HQ molecules in confined water nanopools have an energetically and dynamically different environment from 7HQ molecules in bulk water. Thus, equilibrium between the formation of $T^{\ddagger}$ from T by charge transfer and its reverse reaction (Scheme 1) is suggested to control the dynamics of GSPT.

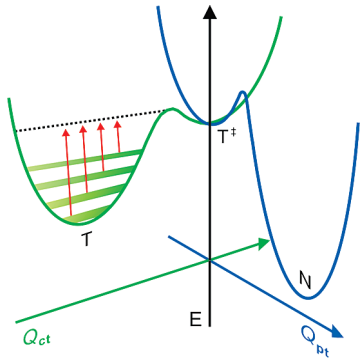

Figure 6. Schematic energetics for the two-step model of 7HQ GSPT in water nanopools of AOT reverse micelles. While Q_{ct} and Q_{pt} denote the coordinates of solvation-coupled charge transfer and proton transfer, respectively, red arrows signify the relative degrees of $\Delta G^{\ddagger}$, which depend on the polarity of local water molecules near 7HQ in a reverse micelle.

To correlate the energetics of the equilibrium with GSPT dynamics, we adopt a continuous solvation model of $k_{PT} = k_{pt} \exp(-\Delta G^{\ddagger}/RT)$, where $\Delta G^{\ddagger}$ is the Gibbs free energy of $T^{\ddagger}$ formation from T.[17,57] In this description, the intrinsic proton transfer of $T^{\ddagger}$, whose isotope-sensitive coordinate is orthogonal to the isotope-insensitive coordinate of charge transfer to form $T^{\ddagger}$, is assumed to take place rapidly via tunneling[8,37] to form N concertedly or stepwise. Consequently, equilibrium to form $T^{\ddagger}$ in the confined water nanopools of reverse micelles becomes energetically unfavorable, reducing the overall proton-transfer rate constant of T. As shown in Table 1, KIE is persistent regardless of w_0 because the overall rate of k_{PT} is determined totally by the rapid charge-transfer equilibrium and KIE originates basically from the intrinsic proton transfer of k_{pt}. Motions of confined water occurring within nanoseconds are still profoundly faster than the overall GSPT observed in microseconds, and the activation energy of GSPT is governed essentially by equilibrated solvation rather than by solvent reorganization motion. In comparison, the retarded solvent motion in the water pool competes with the ESPT of 7HQ to shift the rate-determining step toward the solvent reorganization, so that KIE is reduced. The formation of zwitterionic $T^{\ddagger}$ is unfavorable at low w_0, decreasing k_{PT} and shifting the rate-determining step toward the solvation process. The GSPT dynamics of 7HQ in the water nanopools of reverse micelles is shown schematically in Figure 6, where red arrows signify the relative degrees of $\Delta G^{\ddagger}$. The formation energy of $T^{\ddagger}$ is dependent on the polarity of water molecules near a 7HQ molecule in a reverse micelle. The polarity depends on the relative location from the head groups in a reverse micelle as well as on w_0. Thus, T species experiences a polarity gradient showing a wide Boltzmann distribution in the Gibbs free energy. This dielectric heterogeneity is, as a consequence, reflected by the time-dependent spectral shift of transient T absorption. In an AOT water pool, 7HQ at a more polar environment undergoes GSPT faster than that at a less polar one does. Thus, as time goes by, the relative population of 7HQ molecules at a less polar environment increases, giving birth to the blue shift of the time-resolved transient-absorption spectrum of T as shown in Figure 2. At $w_0 = 12$, the free-energy distribution was deduced to be 420 cm^{-1} (Figure 3). It should be noted that in bulk water, due to homogeneity in polarity, such a large spectral shift has not been reported on the time scale of GSPT.[38]

The reverse tautomerization of 7HQ at the ground state occurs concertedly in the confined water of AOT reverse micelles, as known in alcohols,[23,24] whereas the tautomerization takes place stepwise in bulk water.[37] The rapid decay of an intermediate prototropic species following the slow formation of the intermediate species switches the stepwise mechanism of T tautomerization in bulk water to a concerted mechanism in the polarity-reduced confined water of an AOT reverse micelle. In other words, the altered acid−base energetics of 7HQ prototropic groups and the reduced activity of water render T to undergo GSPT concertedly in the AOT water pool.

5. Conclusions

The GSPT time of 7HQ in confined water nanopools of AOT reverse micelles is several times longer than that in bulk water (26 μs) although it decreases with the size increase of the water nanopool. The $C(t)$ function of transient T absorption decays on the same time scale as the proton transfer time. This suggests that the retardation of proton transfer in water nanopools is due to the increased formation energy of the charge-transferred optimal configuration of $T^{\ddagger}$, which is prerequisite to facile intrinsic proton transfer via tunneling. The coordinates of solvation-coupled charge transfer and proton transfer are considered to be orthogonal to each other. The transient-absorption spectrum of T shifts to the blue with time increment because molecules at a more polar environment undergo GSPT earlier than molecules at a less polar one do. The altered acid−base energetics of 7HQ prototropic groups and the reduced activity of water render T to undergo GSPT concertedly in the AOT water pool.

Acknowledgment. This work was financially supported by research grants through the National Research Foundation of Korea (NRF) funded by the Ministry of Education, Science, and Technology (KRF-2008-313-C00399 and 2009-0082846). We are also thankful to the SRC program of NRF (R11-2007-012-01002-0) while S.Y.P. acknowledges a Seoul fellowship and a BK21 scholarship as well.

References and Notes

(1) (a) Tanner, C.; Manca, C.; Leutwyler, S. *Science* **2003**, *302*, 1736. (b) Fernández-Ramos, A.; Martínez-Núñez, E.; Vázquez, S. A.; Ríos, M. A.; Estévez, C. M.; Merchán, M.; Serrano-Andrés, L. *J. Phys. Chem. A* **2007**, *111*, 5907.
(2) Mohammed, O. F.; Pines, D.; Dreyer, J.; Pines, E.; Nibbering, E. T. J. *Science* **2005**, *310*, 83.
(3) Mohammed, O. F.; Pines, D.; Nibbering, E. T. J.; Pines, E. *Angew. Chem., Int. Ed.* **2007**, *46*, 1458.
(4) Park, S.-Y.; Lee, Y.-S.; Kwon, O.-H.; Jang, D.-J. *Chem. Commun* **2009**, 926.
(5) Inoue, J.; Tomioka, N.; Itai, A.; Harayama, S. *Biochemistry* **1998**, *37*, 3305.
(6) Garczarek, F.; Gerwert, K. *Nature* **2006**, *439*, 109.
(7) Stoner-Ma, D.; Jaye, A. A.; Matousek, P.; Towrie, M.; Meech, S. R.; Tonge, P. J. *J. Am. Chem. Soc.* **2005**, *127*, 2864.
(8) Kwon, O.-H.; Lee, Y.-S.; Yoo, B. K.; Jang, D.-J. *Angew. Chem., Int. Ed.* **2006**, *45*, 415.
(9) Kwon, O.-H.; Lee, Y.-S.; Park, H. J.; Kim, Y.; Jang, D.-J. *Angew. Chem., Int. Ed.* **2004**, *43*, 5792.
(10) Tuckerman, M. E.; Marx, D.; Parrinello, M. *Nature* **2002**, *417*, 925.
(11) Agmon, N. *J. Phys. Chem. A* **2005**, *109*, 13.
(12) Tanner, C.; Thut, M.; Steinlin, A.; Manca, C.; Leutwyler, S. *J. Phys. Chem. A* **2006**, *110*, 1758.
(13) Bach, A.; Coussan, S.; Müller., A.; Leutwyler, S. *J. Chem. Phys.* **2000**, *112*, 1192.
(14) Tolbert, L. M.; Solntsev, K. M. *Acc. Chem. Res.* **2002**, *35*, 19.
(15) Hsieh, C.-C.; Cheng, Y.-M.; Hsu, C.-J.; Chen, K.-Y.; Chou, P.-T. *J. Phys. Chem. A* **2008**, *112*, 8323.
(16) Solntsev, K. M.; Huppert, D.; Agmon, N. *Phys. Rev. Lett.* **2001**, *86*, 3427.
(17) Kwon, O.-H.; Jang, D.-J. *J. Phys. Chem. B* **2005**, *109*, 20479.
(18) Lee, Y.-S.; Yu, H.; Kwon, O.-H.; Jang, D.-J. *Phys. Chem. Chem. Phys.* **2008**, *10*, 153.

(19) (a) Cohen, B.; Huppert, D.; Agmon, N. *J. Phys. Chem. A* **2001**, *105*, 7165. (b) Cohen, B.; Huppert, D. *J. Phys. Chem. A* **2001**, *105*, 2980. (c) Cohen, B.; Leiderman, P.; Huppert, D. *J. Phys. Chem. A* **2002**, *106*, 11115.

(20) (a) Solntsev, K. M.; Huppert, D.; Tolbert, L. M.; Agmon, N. *J. Am. Chem. Soc.* **1998**, *120*, 7981. (b) Tolbert, L. M.; Haubrich, J. E. *J. Am. Chem. Soc.* **1994**, *116*, 10593.

(21) de Bekker, E. J. A.; Pugzlys, A.; Varma, C. A. G. O. *J. Phys. Chem. A* **2001**, *105*, 399.

(22) Mason, S. F.; Philp, J.; Smith, B. E. *J. Chem. Soc. A* **1968**, 3051.

(23) Konijnenberg, J.; Ekelmans, G. B.; Huizer, A. H.; Varma, C. A. G. O. *J. Chem. Soc., Faraday Trans. 2* **1989**, *85*, 39.

(24) Itoh, M.; Adachi, T.; Tokumura, K. *J. Am. Chem. Soc.* **1984**, *106*, 850.

(25) Park, S.-Y.; Lee, Y.-S.; Jang, D.-J. *Phys. Chem. Chem. Phys.* **2008**, *10*, 6703.

(26) Chou, P.-T.; Wei, C.-Y.; Wang, C.-R. C.; Hung, F.-T.; Chang, C.-P. *J. Phys. Chem. A* **1999**, *103*, 1939.

(27) Chou, P.-T.; Wei, C.-Y. *J. Phys. Chem. B* **1998**, *102*, 3305.

(28) Angulo, G.; Organero, J. A.; Carranza, M. A.; Douhal, A. *J. Phys. Chem. B* **2006**, *110*, 24231.

(29) Douhal, A.; Angulo, G.; Gil, M.; Organero, J. A.; Sanz, M.; Tormo, L. *J. Phys. Chem. B* **2007**, *111*, 5487.

(30) Bach, A.; Tanner, C.; Manca, C.; Frey, H.-M.; Leutwyler, S. *J. Chem. Phys.* **2003**, *119*, 5933.

(31) Meuwly, M.; Bach, A.; Leutwyler, S. *J. Am. Chem. Soc.* **2001**, *123*, 11446.

(32) Kwon, O.-H.; Doo, H.; Lee, Y.-S.; Jang, D.-J. *ChemPhysChem* **2003**, *4*, 1079.

(33) Kwon, O.-H.; Kim, T. G.; Lee, Y.-S.; Jang, D.-J. *J. Phys. Chem. B* **2006**, *110*, 11997.

(34) Park, H. J.; Kwon, O.-H.; Ah, C. S.; Jang, D.-J. *J. Phys. Chem. B* **2005**, *109*, 3938.

(35) Yu, H.; Kwon, O.-H.; Jang, D.-J. *J. Phys. Chem. A* **2004**, *108*, 5932.

(36) Kim, T. G.; Kim, Y.; Jang, D.-J. *J. Phys. Chem. A* **2001**, *105*, 4328.

(37) Kim, T. G.; Lee, S.-I.; Jang, D.-J.; Kim, Y. *J. Phys. Chem.* **1995**, *99*, 12698.

(38) Lee, S.-I.; Jang, D.-J. *J. Phys. Chem.* **1995**, *99*, 7537.

(39) Poizat, O.; Bardez, E.; Buntinx, G.; Alain, V. *J. Phys. Chem. A* **2004**, *108*, 1873.

(40) Bardez, E.; Châtelain, A.; Larrey, B.; Valeur, B. *J. Phys. Chem.* **1994**, *98*, 2357.

(41) (a) Bardez, E.; Fedorov, A.; Berberan-Santos, M. N.; Martinho, J. M. G. *J. Phys. Chem. A* **1999**, *103*, 4131. (b) Bardez, E.; Devol, I.; Larrey, B.; Valeur, B. *J. Phys. Chem. B* **1997**, *101*, 7786.

(42) Bardez, E.; Monnier, E.; Valeur, B. *J. Phys. Chem.* **1985**, *89*, 5031.

(43) Bhattacharyya, K. *Acc. Chem. Res.* **2003**, *36*, 95.

(44) Nandi, N.; Bhattacharyya, K.; Bagchi, B. *Chem. Rev.* **2000**, *100*, 2013.

(45) (a) Cohen, B.; Huppert, D.; Solntsev, K. M.; Tsfadia, Y.; Nachliel, E.; Gutman, M. *J. Am. Chem. Soc.* **2002**, *124*, 7539. (b) Piletic, I. R.; Moilanen, D. E.; Spry, D. B.; Levinger, N. E.; Payer, M. D. *J. Phys. Chem. A* **2006**, *110*, 4985. (c) Spry, D. B.; Glusac, G. K.; Moilanen, D. E.; Fayer, M. D. *J. Am. Chem. Soc.* **2007**, *129*, 8122.

(46) Kalyanasundaram, K. *Photochemistry in microheterogeneous systems*; Academic Press: Orlando, FL, 1987.

(47) Dutta, P.; Sen, P.; Mukherjee, S.; Halder, A.; Bhattacharyya, K. *J. Phys. Chem. B* **2003**, *107*, 10815.

(48) Maitra, A. *J. Phys. Chem.* **1984**, *88*, 5122.

(49) Hauser, H.; Haering, G.; Pande, A.; Luisi, P. L. *J. Phys. Chem.* **1989**, *93*, 7869.

(50) Venables, D. S.; Huang, K.; Schmuttenmaer, C. A. *J. Phys. Chem. B* **2001**, *105*, 9132.

(51) Park, S.; Moilanen, D. E.; Fayer, M. D. *J. Phys. Chem. A* **2008**, *112*, 5279.

(52) Hazra, P.; Chakrabarty, D.; Sarkar, N. *Langmuir* **2002**, *18*, 7872.

(53) Riter, R. E.; Willard, D. M.; Levinger, N. E. *J. Phys. Chem. B* **1998**, *102*, 2705.

(54) Moilanen, D. E.; Levinger, N. E.; Spry, D. B.; Fayer, M. D. *J. Am. Chem. Soc.* **2007**, *129*, 14311.

(55) Balasubramanian, S.; Pal, S.; Bagchi, B. *Phys. Rev. Lett.* **2002**, *89*, 115505.

(56) Faeder, J.; Ladanyi, B. M. *J. Phys. Chem. B* **2005**, *109*, 6732.

(57) Mente, S.; Maroncelli, M. *J. Chem. Phys.* **1998**, *102*, 3860.

(58) Maroncelli, M.; Fleming, G. R. *J. Chem. Phys.* **1987**, *86*, 6221.

(59) Politi, M. J.; Chaimovich, H. *J. Phys. Chem.* **1986**, *90*, 282.

(60) Hasegawa, M.; Sugimura, T.; Suzuki, Y.; Shindo, Y.; Kitahara, A. *J. Phys. Chem.* **1994**, *98*, 2120.

(61) Berger, C. L.; Svensson, E. C.; Thomas, D. D. *Proc. Natl. Acad. Sci. U.S.A.* **1989**, *86*, 8753.

(62) Cho, C. H.; Urquidi, J.; Singh, S.; Robinson, G. W. *J. Phys. Chem. B* **1999**, *103*, 1991.

JP903693F